Journal of Forestry Research (2011) 22(3): 437–446
DOI 10.1007/s11676-011-0185-5

ORIGINAL PAPER

Future impacts of climate change on forest fire danger in northeastern China

TIAN Xiao-rui • SHU Li-fu • ZHAO Feng-jun • WANG Ming-yu • Douglas J. McRae

Received: 2010-09-07; Accepted: 2010-11-10

Abstract: Climate warming has a rapid and far-reaching impact on forest fire management in the boreal forests of China. Regional climate model outputs and the Canadian Forest Fire Weather Index (FWI) System were used to analyze changes to fire danger and the fire season for future periods under IPCC Special Report on Emission Scenarios (SRES) A2 and B2, and the data will guide future fire management planning. We used regional climate in China (1961–1990) as our validation data, and the period (1991–2100) was modeled under SRES A2 and B2 through the weather simulated by the regional climate model system (PRECIS). Meteorological data and fire danger were interpolated to 1 km^2 by using ANUSPLIN software. The average FWI value for future spring fire seasons under Scenarios A2 and B2 shows an increase over most of the region. Compared with the baseline, FWI averages of spring fire season will increase by –0.40, 0.26 and 1.32 under Scenario A2, and increase by 0.60, 1.54 and 2.56 under Scenario B2 in 2020s, 2050s and 2080s, respectively. FWI averages of autumn fire season also show an increase over most of the region. FWI values increase more for Scenario B2 than for Scenario A2 in the same periods, particularly during the 2050s and 2080s. Average future FWI values will increase under both scenarios for autumn fire season. The potential burned areas are expected to increase by 10% and 18% in spring for 2080s under Scenario A2 and B2, respectively. Fire season will be prolonged by 21 and 26 days under Scenarios A2 and B2 in 2080s respectively.

Keywords: climate change; fire season; forest fire danger; northeastern China

Foundation project: This work was financially support by National Science and Technology Support Plan (2007BAC03A02) and National Natural Science Foundation of China (30671695)
The online version is available at http://www.springerlink.com

TIAN Xiao-rui (✉) • SHU Li-fu • ZHAO Feng-jun • WANG Ming-yu
State Forestry Administration's Key Open Laboratory of Forest Protection; Research Institute of Forest Ecology, Environment and Protection, Chinese Academy of Forestry, Beijing 100091. E-mail: tianxr@caf.ac.cn

Douglas J. McRae
Natural Resources Canada, Canadian Forest Service, 1219 Queen St. E. Sault Ste. Marie, Ontario P6A 2E5.

Responsible editor: Yu Lei

Introduction

Forest fire is the dominant disturbance regime in boreal forests. It is the primary process, which organizes the physical and biological attributes of the boreal biome over most of its range, shaping landscape diversity and influencing energy flows and biogeochemical cycles, particularly the global carbon cycle since the last Ice Age (Weber and Flannigan 1997; Soja et al. 2006). Climate change over the next 100 years is expected to have significant impacts on forest ecosystems. The temporal and spatial dynamics of fire are likely to be altered as climate continues to change. Wildland fire is a global phenomenon, and a result of interactions between climate and weather, fuels, and people. Weather and climate are the most important factors influencing fire activity and these factors are changing due to human-caused climate change (Flannigan et al. 2005). The forestry community needs to evaluate the long-term effects of climate change on forests and determine what the community might do now and in future to respond to this threat (Spittlehouse 2003).

There is substantial evidence throughout the boreal region to conclude that the biosphere within the boreal terrestrial environment has already responded to the transient effects of climate change. In Siberia, in seven of the last nine years there were extreme fire seasons, and extreme fire years were more frequent in both Alaska and Canada (Soja et al. 2006). The change in temperature increase and warming is faster than that predicted in some regions. In forest region of Inner Mongolia, Zhao et al. (2009) found that mean temperature increased, and fire occurrence dates extended into summer during 1980 to 2006. A similar change occurred in Yichun, Heilongjiang, where forest fire frequency showed an increasing trend due to increased temperature and decreased rainfall during 1961 to 2003 (Gao et al. 2008). Many studies addressed the impact of climate change on fire frequency. Flannigan et al. (2009) reviewed the current under-

standing of what the future may bring with respect to wildland fire. Research results predict a general increase in area burned and fire occurrence in future, but there will be substantial spatial variability, with some areas of no change or even decreases in area burned and frequency (Flannigan et al. 2009). Fire seasons are lengthening for temperate and boreal regions, and this trend should continue in a warmer world (Flannigan et al. 2009). Recent studies suggest a doubling of area burned along with a 50% increase in fire occurrence in parts of the boreal zone by the end of this century (Flannigan et al. 2009). Wotton and Flannigan (2010) used the Canadian Climate Centre general circulation models (GCM) to predict an increase in fire frequency of 25% by 2030 and 75% by the end of the 21st century overall across Canada. But the predictions from fire climate scenarios derived from the Hadley Centre GCM suggest fire frequency will increase by 140% by the end of this century. Future climate change would trigger weather conditions more favorable to forest fires and a slight increase in regional (Waswanipi area, central Quebec) fire activity (+7%) (Le Goff et al. 2009). Under the A2 climate change scenario, the fire risk in August would double (+110%) for 2100, while that in May would decrease slightly (-20%), moving the fire season peak later in the season (Le Goff et al. 2009). Under a 2 × CO_2 scenario, future area burned is predicted to increase 478% for Portugal as a whole, which equates to an increase from 1.4% to 7.8% of the available burnable area burning annually. Fire occurrence showed a dramatic increase (279%) for all of Portugal (Carvalho et al. 2010). The increases in temperature are predicted to lead to an increase in the annual mean area burned in western United States by 54% by the 2050s. Changes in area burned are ecosystem dependent, with the forests of the Pacific Northwest and Rocky Mountains experiencing the greatest increases of 78 and 175%, respectively (Spracklen et al. 2009). All future scenarios show an increase in mean monthly temperature maxima and one model scenario forecasts an increase in dry spell sequences, resulting in a slight increase in forecasted annual area burned in the Great Lakes-St Lawrence forest of Canada (Drever et al. 2009). Compared to data from 1991 to 2000, the average area burned per decade across Alaska and western Canada will double by 2041 to 2050, and will increase on the order of 3.5–5.5 times by the last decade of the 21st century (Balshi et al. 2008). Under the 2 × CO_2 and 3 × CO_2 scenarios, there will be a relative increase in area burned in northern Alberta of 12.9%–29.4% from the reference 1 × CO_2 scenario (Tymstra et al. 2007). The longer, warmer and drier summer seasons predicted to result from climate change are expected to increase the frequency and intensity of forest fires in the Northwest Territories of Canada by the end of the 21st century (Kochtubajda et al. 2006). The combined frequencies of days with very high and extreme Forest Fire Danger Index (FFDI) ratings in Southeastern Australia would be likely to increase by 4%–25% by 2020 and by 15%–70% by 2050 (Hennessy et al. 2005). The window available for prescribed burning may be shifted and narrowed. Yang et al. (2010) analyzed the climate change in Daxing'an Moutains of northeast China for future periods and forecasted that the burned area would double in the 21st century under IPCC SRES A2a and B2a scenarios based on a linear regression model between the mean seasonal severity rating (SSR) values and burned areas. A people-caused fire prediction model, combined with GCM data predicted the total number of people-caused fires in Ontario could increase by approximately 18% by 2020–2040 and 50% by the end of the 21st century (Wotton et al. 2003). The emissions of greenhouse gases from all Canadian fires are predicted to increase from about 162 $Tg{\cdot}a^{-1}$ of CO_2 equivalent in the 1 × CO_2 scenario to 313 $Tg{\cdot}a^{-1}$ of CO_2 equivalent in the 3 × CO_2 scenario, including contributions from CO_2, CH_4 and N_2O (Amiro et al. 2009).

The global climate has been warming over the past 100 years in China. Annual average surface temperature increased by about 0.5–0.8°C. In northern China the climate changed significantly over the past 50 years. Warming occurs mainly during the winter and spring periods, while the annual precipitation did not show any significant change except for larger decadal fluctuations (Qin et al. 2005; Tang et al. 2005). Most large forest fires occurred in this area of China. Forest fire occurrence is highly discrete in temporal distribution. Usually, a large number of fires occur simultaneously in a short time period under extreme fire weather conditions. Regional climate model output and the calculated FWI System are used to analyze the influence of climate change on fire danger in northeast China at a scale of 2500 km^2. Canadian Forest Fire Danger Rating System (Stocks et al. 1989) can be effectively used in northeast China to forecast fire occurrence, fire behavior, and fire impacts (Lynham and Stocks 1989; Tian et al. 2010). Analyzing changes in forest fire danger for future periods under the IPCC SRES A2 and B2 scenarios will help government to improve forest fire management planning for northeastern China.

Methodology

Overview of the study area

The study area (38.72° N–53.56° N, 115.53° E–135.08° E) is located in northeastern China including Heilongjiang, Jilin, and Liaoning provinces, and eastern Inner Mongolia (Fig. 1). The landscape of northeast China consists of mountains in the east (Changbai Mountain) and west (Daxing'an Mountains) with a plain (northeast plain) in the middle. The average altitude of the mountainous areas is 1 000 m ASL, while the central plains average 200 m ASL.

China's largest natural forest areas are mainly located in this region in the Daxing'an Mountains and Xiaoxing'an Mountains in Heilongjiang Province and Changbai Mountain in Jilin Province. The main forest type in the region is the temperate coniferous-deciduous broad-leaved mixed forest. There is a total of 45.33 million hectares forest area in the region, accounting for 37% of the total forest area in China. Forest areas in northeast China can be roughly divided into three parts: Daxing'an Mountains, Xiaoxing'an Mountains, and Changbai Mountain forest region. The Daxing'an Mountains, located in northwestern Heilongjiang Province and northeastern Inner Mongolia, has *Larix gmelinii*, *Pinus sylvestris*, *Pinus koraiensis*, *Betula platyphylla*,

Quercus mongolicus, *Populus davidiana*, *Tilia tuan*, *Juglans mandshurica*, and *Fraxinus mandshurica* as the main forest species. Larch forest covers 86.1% of the forest area in the Daxing'anling Region. The Xiaoxing'an Mountains is located in the northern part of Heilongjiang Province, an area about four million hectares, with tree species similar to those in the Daxing'an Moutains, but with more Korean pine forest and less larch forest. Changbai Mountain is located in eastern Jilin Province, where the main vegetation type is temperate mixed forest. Tree species at Changbai Mountain include *Pinus koraiensis*, *Larix gmelinii*, *Picea asperata*, *Abies holophylla* and *Pinus densiflora*.

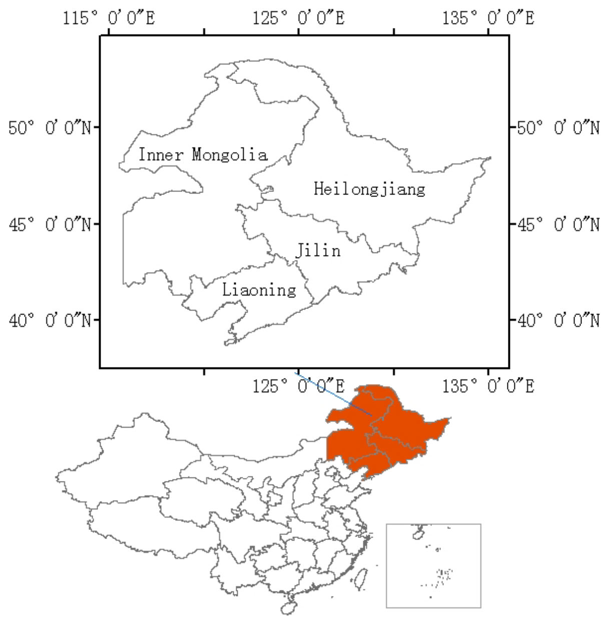

Fig. 1 Location of the study area in northeastern China

The study area is characterized by a cool temperate continental monsoon climate with four seasons and an average annual temperature range of 5–10°C. The frost-free period is about 150 days. There is a large difference in temperatures from north to south, and precipitation declines from east to west. In spring (March – May) temperatures warm rapidly with strong winds and drought. Annual precipitation is 400–700 mm in most of the region, and up to 1 000 mm in the southeast at Changbai Mountain. About 70% of the precipitation is concentrated in the summer (Sun et al. 2006). The zonal soils are lime soil, tundra soil, and dark brown soil in the colder boreal zone, and dark brown soil, black soil and chernozem in the temperate zone (Zhong 1990).

The study area has historically been affected by large and frequent forest fires. During 1999–2007, there were 5 689 fires accounting for 7.3% of all fires in China, and the burned area covered 2 266 226 ha area, accounting for 73.8% of the total burned area in the country. Major fire causes in the area are lightning and man-made fire. Around 57% of fires were caused by lightning in the Daxing'an Moutains range (Tian et al. 2009).

Data sources

Data for the climate scenarios in this paper were extracted from the regional climate model Providing Regional Climate for Impact Studies (PRECIS) (Johns et a1. 2004; Xu et al. 2006). Historical regional climate data for the baseline period of 1961−1990 in China are from the China Meteorological Data and Sharing Network (http://cdc.cma.gov.cn/). There are 685 weather stations in the entire country and 107 in the study area. ANUSPLIN software (Hutchinson 1998) was used to interpolate meteorological data to 1 km × 1 km raster data.

Calculation of forest fire weather index

The FWI System input for weather observations is at solar noon every day. All FWI System components were calculated based on regional climate model daily outputs at a scale of 50 × 50 km. Since the FWI System works on the basis of solar noon weather parameters, temperature was estimated by subtracting 2°C from the daily maximum temperature (Williams et al. 2001). Rainfall was estimated from PRECIS output. Since regional climate models usually output only daily average relative humidity, Equ. (1) was used to derive minimum relative humidity from daily average relative humidity. The relationship between minimum relative humidity and the daily average humidity was estimated based on data for the baseline period from all 685 national weather stations as:

$$RH_{\min} = 0.2053RH_{ave} - 0.2308Mon \quad R = 0.83 \qquad (1)$$

Where, $RH_{\min}$ and RH_{ave} are the minimum relative humidity and daily average relative humidity, respectively, and *Mon* is the number of the month. Wind speed was estimated based on regional climate model output for daily average wind speed.

Daily fuel moisture codes and fire behavior indices for the FWI System were calculated from daily weather estimates for every grid cell under the two climate scenarios for the period 1960–2100. Codes and indices were averaged for the month in the fire season. The average FWI estimates for periods were interpolated to a scale of 1 × 1 km by using the software Anusplin.

Results

Two peaks in the fire season were observed for our study area, a spring season peak from March to May and an autumn season peak in October. According to the statistics of 2003–2005 from local fire agencies, 76.6% of the fires occurred in the spring fire season and covered 75.6% of the annual burned area. Autumn fires accounted for 6.3% of all fires, but 22.3% of the area burned annually. In this bimodal fire season, 82.9% of fires accounted for 97.9% of the total annual burn area. This result showed that our analysis should focus on fire danger changes based on the two fire peak seasons and three future periods under two climate scenarios.

Climate change in future periods

Temperature and precipitation are two important factors that affect climate, and they are naturally the factors of greatest concern for future climate change analyses. The simulated average temperature and monthly precipitation in spring fire peak season from the PRECIS model were 3.1°C (range −8.2 to 10.9°C), and 24.1 mm (range 7.4–67.3 mm). The two predicted means closely approximated observed values of 3.2°C and 23.7 mm. In autumn fire season the observed average temperature and monthly precipitation were 3.1°C (range −8.0 to 14.6°C) and 22.9 mm (range 3.3–51.3 mm), and the simulated values were 3.3°C (range −8.6 to 14.1°C) and 22.3 mm (range 7.1–51.4 mm). The simulated results also closely approximated observed spatial distributions, indicating that PRECIS was accurate in predicting temperature and precipitation.

The average temperature of northeastern China in spring and autumn fire seasons were 2.87°C and 3.13°C during the baseline period, respectively. The means are predicted to increase by 0.29°C, 0.78°C and 1.62°C, respectively, in 2020s (2011–2030), 2050s (2041–2060) and 2080s (2071–2100) under scenario A2, and by 0.54°C, 0.92°C and 1.32, respectively, under scenario B2 (Fig. 2). Precipitation on the study area is predicted to increase by 2.7 mm, 6.3 mm, and 11.8 mm under scenarios A2, and 2.0 mm, 2.6 mm and 1.9 mm under scenarios B2 in 2020s, 2050s and 2080s, respectively, compared with the baseline period (71.8 mm). For autumn fire season, the mean temperatures of the study area are predicted to increase by 1.00°C, 2.37°C and 4.58°C, and increase by 1.21°C, 2.25°C and 3.56°C under scenario B2, respectively. Precipitation during the autumn fire season in the baseline period was 22.0 mm, and it is predicted to increase by 1.3 mm, 3.3 mm and 5.0 mm under scenario A2, and 0.2 mm, 0.8 mm and -0.1 mm under scenario B2 in 2020s, 2050s and 2080s, respectively.

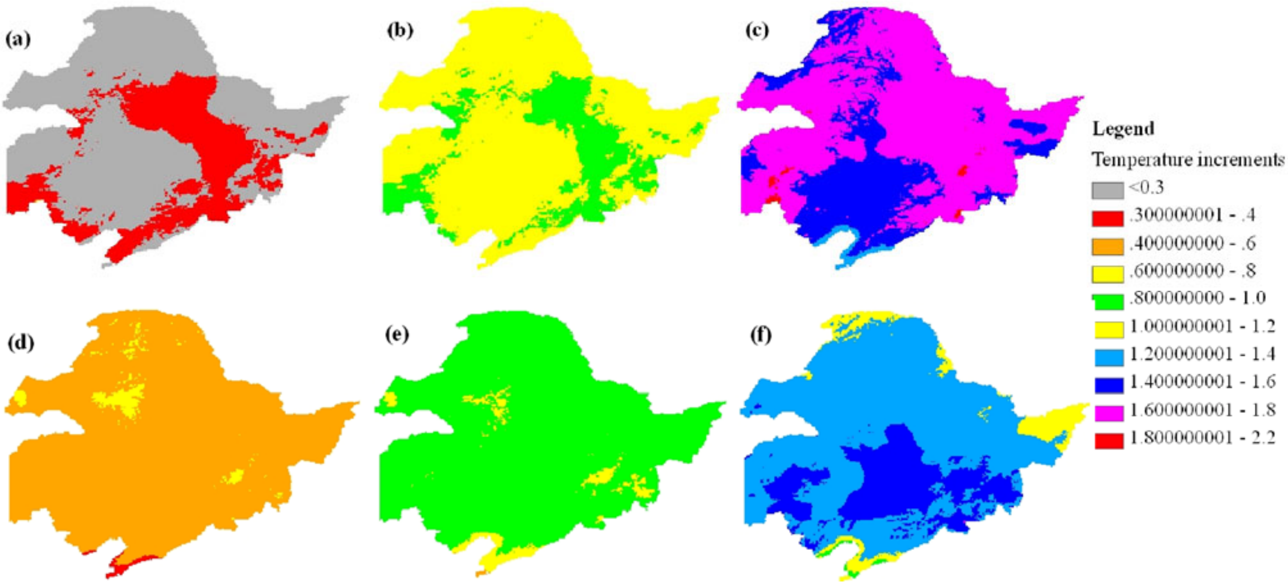

Fig. 2 Temperature increments in spring fire season for the future periods: (a) Scenario A2 for the 2020s; (b) Scenario A2 for the 2050s; (c) Scenario A2 for the 2080s; (d) Scenario B2 for the 2020s; (e) Scenario B2 for the 2050s; and (f) Scenario B2 for the 2080s.

Changes of fire danger in future periods

During the baseline period in northeast China, FWI in the spring and autumn fire peak seasons showed a decreasing trend from southwest to northeast (Fig. 3). FWI values were high in the spring fire season, ranging from 4 to 18 in most parts of the region, but they were relatively low ranging from 2 to 10 in October.

The future average FWI during spring fire season was predicted to generally increase in our simulation modeling under Scenarios A2 and B2 (Fig. 4). There were small decreases in some areas. Under Scenario A2, spring FWI averages would decrease initially by -0.40 in the 2020s, but then increase by 0.26 and 1.32 in the 2050s and 2080s, respectively, compared with the baseline period. The average monthly FWI would decrease in March by −1.49, −1.36, and −0.97, but would increase in May by 1.13, 2.52, and 4.52 in the 2020s, 2050s and 2080s, respectively. The average FWI in April would decrease slightly in 2020s and 2050s, but would increase in 2080s.

Associated with FWI changes, there will also be spatial distribution changes. In the 2020s, the average FWI value would decrease by from −5.14 to 2.68 in the western portion of the study area. By the 2050s, the FWI values would increase significantly in most parts of the region except the southeast. The east-central part of the region would see the highest FWI during the 2080s with an increase of more than 2.0.

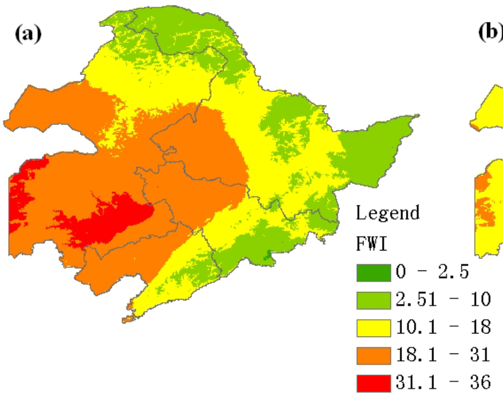

Fig. 3 Average FWI for Northeastern China and autumn for the baseline period.
(a) spring (March-May) fire season; and (b) autumn (October) fire season

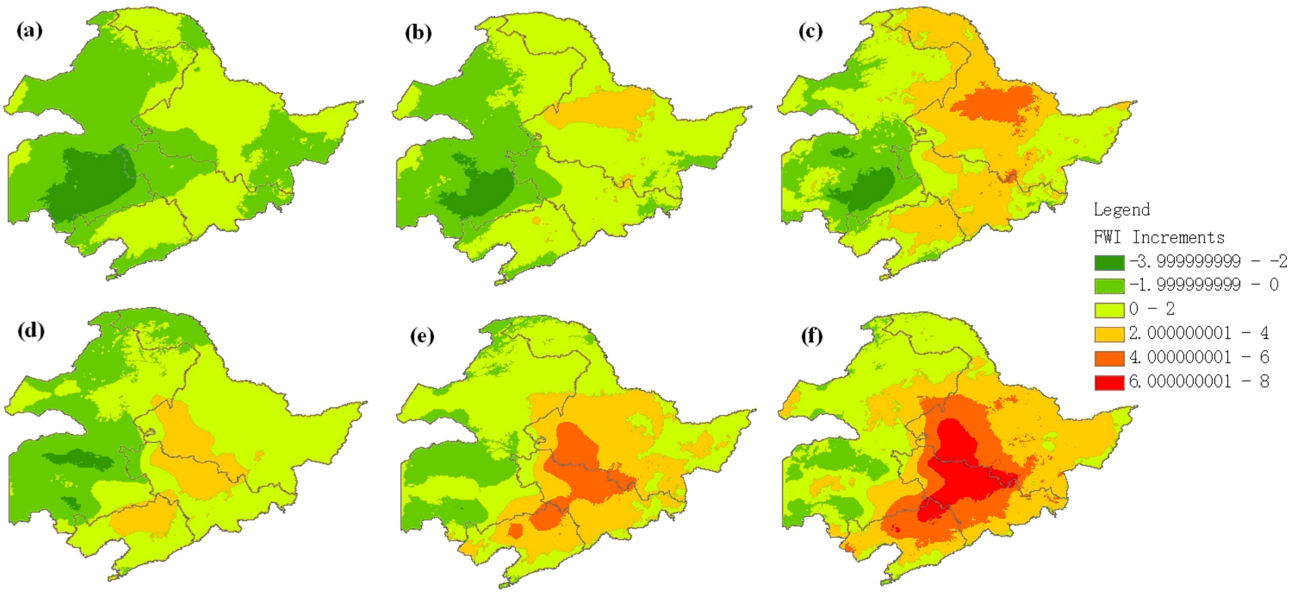

Fig. 4 Changes in the mean FWI of spring fire season under Scenarios A2 and B2. (a) Scenario A2 for the 2020s; (b) Scenario A2 for the 2050s; (c) Scenario A2 for the 2080s; (d) Scenario B2 for the 2020s; (e) Scenario B2 for the 2050s; and (f) Scenario B2 for the 2080s.

Under Scenario B2, the average FWI values for the spring fire season in 2020s, 2050s and 2080s would increase by 0.60, 1.54 and 2.56, respectively, compared with the baseline period. Average FWI values would increase in April and May of the three forecast periods compared with baseline period, but will decreased in March in the 2020s and 2050s. Average FWI values would show the largest increase in May, 1.76, 3.42, and 5.07 in the 2020s, 2050s and 2080s, respectively.

Under Scenario B2, regions with largest FWI increase showed a similar spatial distribution, which increased greatly in the central part while slightly increasing or decreasing in the west (Fig. 4). The average increase of the FWI under Scenario B2 would be greater than that over the same period under Scenario A2. In particularly, FWI values would increase detectably during the 2050s and 2080s under Scenario B2.

Under Scenario A2 and B2, average FWI values in October in future would increase compared to the baseline period. Under Scenario A2, FWI averages would increase by 0.23, 0.59, and 1.27 in the 2020s, 2050s and 2080s, respectively. Under Scenario B2, FWI averages would increase by 1.09, 1.83, and 2.55 in the 2020s, 2050s and 2080s, respectively. For Scenario A2 during the 2020s, there would be a FWI increase (Fig. 5) in the eastern study area, but in the 2050s and 2080s there would be a relatively large FWI increase in the northern and southern parts. FWI would increase greatly from northwest to southeast of the study area under Scenario B2, which is different from the prediction of Scenario A2 (Fig. 5). In the southeastern part there would be a larger increase of fire danger.

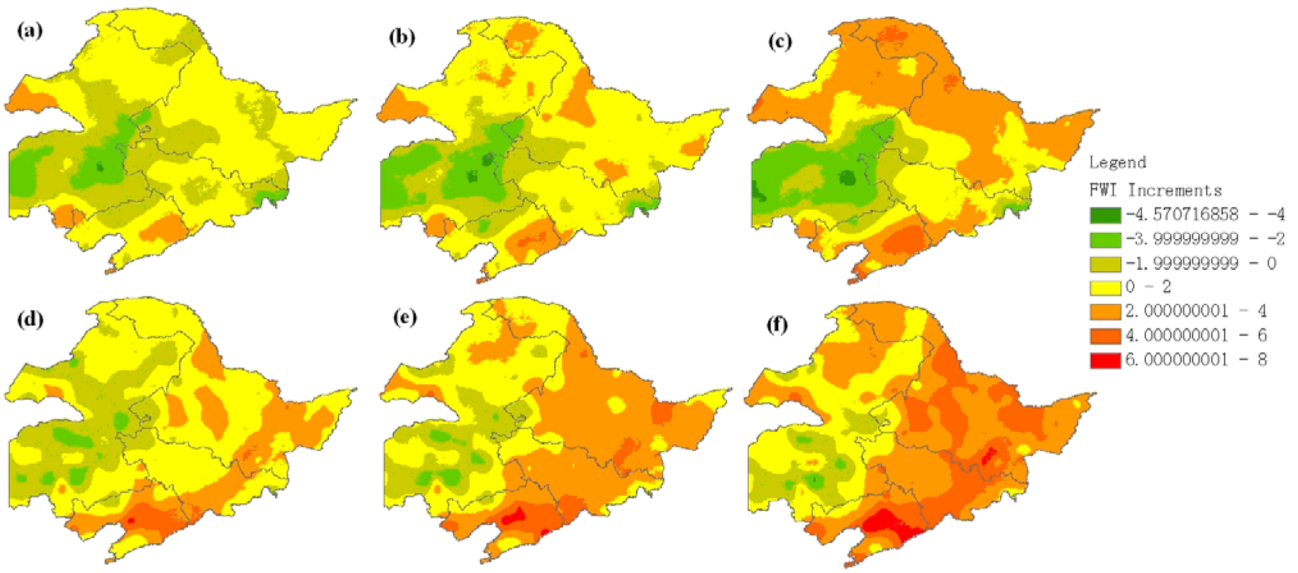

Fig. 5 Changes in the mean FWI of October under Scenarios A2 and B2. (a) Scenario A2 for the 2020s; (b) Scenario A2 for the 2050s; (c) Scenario A2 for the 2080s; (d) Scenario B2 for the 2020s; (e) Scenario B2 for the 2050s; and (f) Scenario B2 for the 2080s.

Changes of potential burned areas

The FWI System is correlated to area burned, and the ratio of FWI is a better index of the relationship between fire danger and potential burned areas. Statistical data covering several decades suggested approximately a one-to-one relationship between FWI and area burned (Harrington et al. 1983; Wittrock & Wheaton 1997). For example, if FWI increases by 50% for a scenario simulation we could expect a similar increase in area burned (Flannigan, et al. 2001). Under scenario A2, the average FWI ratios were 0.97, 1.01, and 1.10 during spring fire season, and 1.06, 1.12, and 1.23 during autumn fire season in 2020s, 2040s and 2080s, respectively (Fig. 6 and Fig. 7). These values indicate the potential burned area would show a slight change in the 2020s and 2040s, but increase by 23% in the 2080s. Most of the increase for October in the 2080s would occur in the northern (including Danxing'anling) and southern parts of the study area (Fig. 7).

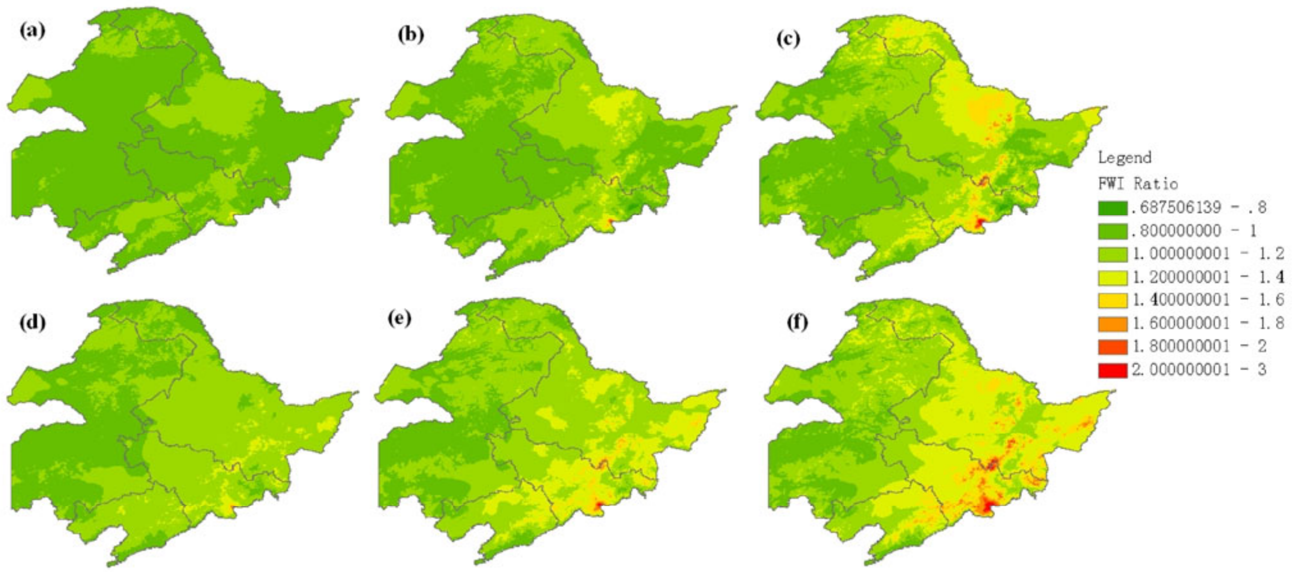

Fig. 6 FWI ratio for Spring fire season under SERS A2 and B2 scenarios. (a) Scenario A2 for the 2020s; (b) Scenario A2 for the 2050s; (c) Scenario A2 for the 2080s; (d) Scenario B2 for the 2020s; (e) Scenario B2 for the 2050s; and (f) Scenario B2 for the 2080s.

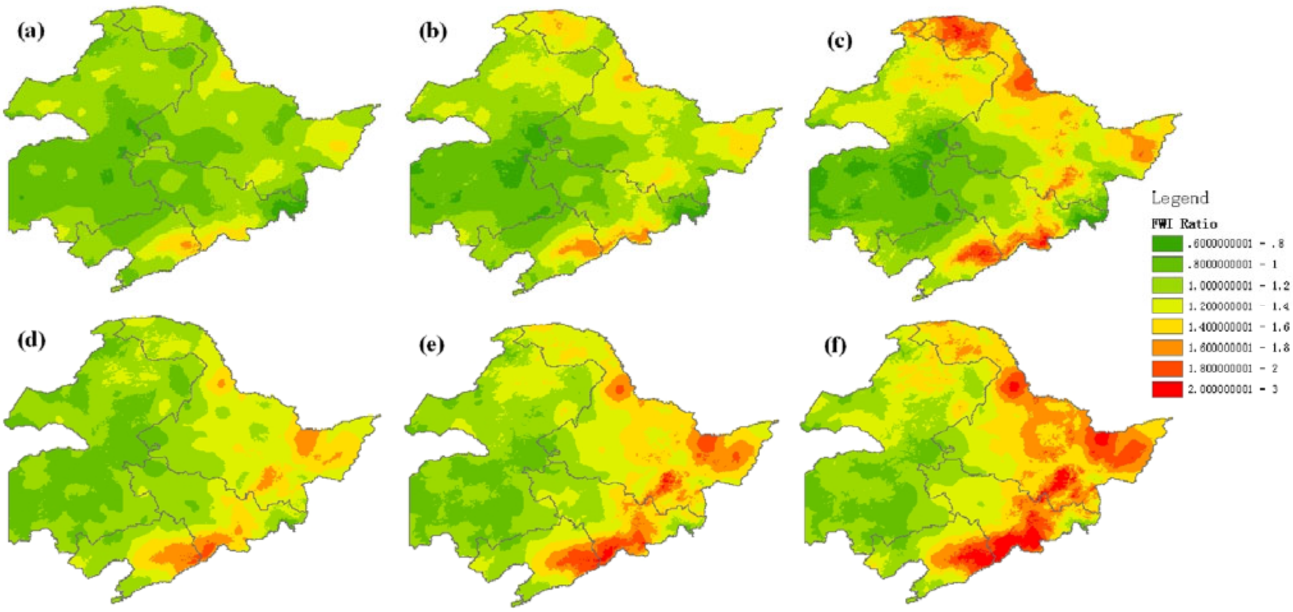

Fig. 7 FWI ratio for October under SERS A2 and B2 scenarios. (a) Scenario A2 for the 2020s; (b) Scenario A2 for the 2050s; (c) Scenario A2 for the 2080s; (d) Scenario B2 for the 2020s; (e) Scenario B2 for the 2050s; and (f) Scenario B2 for the 2080s.

Under scenario B2, the average FWI ratios were 1.04, 1.11, and 1.18 during spring fire season, and 1.17, 1.26, and 1.35 during autumn fire season for the 2020s, 2040s and 2080s, respectively. The potential burned areas would increase by 4%–18% during spring fire season and 17%–35% in autumn. Under scenario B2, there would be a great increase in burned area in the southeastern part of the study area (eg: Changbai Mountains).

Change of fire season

In Northeast China, the low, medium, high, very high and extreme fire danger ratings were found to correspond to a FWI range of 0–2.5, 2.6–10.0, 10.1–18.0, 8.1–31.0, and >31.0, respectively (Tian et al. 2009). Fire danger decreased gradually from southwest to northeast for the baseline period (Fig. 3). The number of days with extreme fire danger rating ranged from 46 to 66 in the western region but only 1–25 days in the east. In the Daxing'anling, 77.5% of all fires occur at FWI levels in the high fire danger class or higher (Tian et al. 2009). In the western region, there were 126–171 days in this broad FWI class, while in the east there were only 1–50 days. But the main land uses are farmland or wildland in the central and west parts of the study area, and these land use classes typically have low forest fire risk.

Compared with the baseline period, fire season (the days with high or higher fire danger rating) would increase significantly in future under Scenarios A2 and B2 (Table 1). In the 2080s under Scenario A2, the number of days of high, very high, and extreme fire danger would, on average, increase by 1, 6, and 14 days, respectively in the study area. Under Scenario B2 for the 2080s, the number of days with high and higher fire danger rating would increase more significantly, with 0, 5, and 21 days in the high, very high and extreme fire danger rating classes, respectively.

Table 1. Future fire season changes based on days at higher fire danger classes for northeast China under Scenarios A2 and B2

Scenarios	Periods	Fire danger rating classes (FWI)			
		High	Very High	Extreme	Total
	Baseline	52	47	46	145
A2	2020s	-2	0	3	1
	2050s	-1	2	7	8
	2080s	1	6	14	21
B2	2020s	-1	1	9	9
	2050s	0	3	14	17
	2080s	0	5	21	26

In the eastern part of the study area the increasing days with high or higher fire danger rating would be more apparent than in the western region. Under Scenario A2 in the 2020s, the number of the days with high and higher fire danger rating would increase by 1–16 days in the east, while decreasing by 1–14 days in the west compared to the baseline period (Fig. 8). By the 2050s and 2080s, the number of days with high or higher fire danger rating would decrease by 1–13 days in the west and increase in the east. Especially in the 2080s, the number of days with high or higher fire danger rating would increase by more than 20 days in the Daxing'an Mountains and Xiaoxing'an Mountains, and 41–60 days in the Changbai Mountain.

Under Scenario B2, the increase of days with high or higher fire danger rating would be more than predicted for the same period under Scenario A2. The spatial distribution of these increases would be similar with that found for Scenario A2. Significant increases in the number of days with high or higher fire

danger rating would be mainly distributed in the southeast region under Scenario B2.

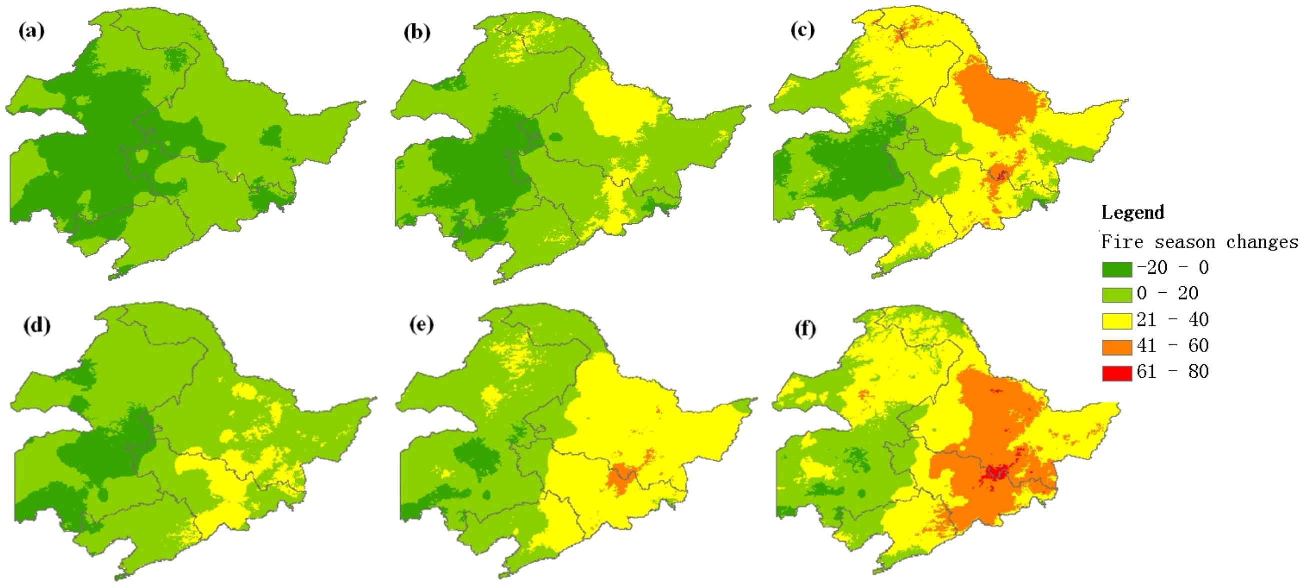

Fig. 8 Fire season changes under Scenarios A2 and B2. (a) Scenario A2 for the 2020s; (b) Scenario A2 for the 2050s; (c) Scenario A2 for the 2080s; (d) Scenario B2 for the 2020s; (e) Scenario B2 for the 2050s; and (f) Scenario B2 for the 2080s.

Conclusion and discussion

Both scenarios A2 and B2 predicted increases in average FWI values for the spring fire season over most of northeastern China with only a few small areas showing declines. The east-central part of the region would have the greatest FWI values by the 2080s. Under Scenario B2, the regions with large increases in FWI would have similar spatial distributions with those under Scenario A2, but with significant increases in the southeastern portion of the region. The average increase of FWI under Scenario B2 would be greater than the increase for the same period under Scenario A2, particularly in the 2050s and 2080s.

Under Scenarios A2 and B2, the average October FWI values in future would increase over the baseline period. Under Scenario A2 the values in the southwestern part of the region would show obvious increases in the FWI of the 2020s, but this would be more generally spread throughout the region by the 2050s and 2080s. However, there would be little change in the FWI for the central part during these periods.

Compared with the baseline period, fire season would increase significantly in future periods under Scenarios A2 and B2. Regions with an obvious increase would be mainly located in the southeast and northwest areas.

The potential burned areas are expected to increase by 10% and 23%, respectively, in 2080s under scenario A2 in the spring and autumn fire seasons, and increase by 18% and 35% under scenario B2. Yang et al. (2010) predicted the area burned would peak in the 2080s under both A2a and B2a scenarios, and area burned would increase by 20%–85% in the spring fire season under the A2a scenario and 27%–65% under the B2a scenario in Daxing'an Mountains. These results are basically consistent although different scenarios were used. The application of the PRECIS regional climate model provided us with good simulation capability for modeling daily average temperature and monthly precipitation for northeastern China over the fire season. Validation using data from 1961 to 1990 showed predictions were very similar to historic data in terms of amounts and spatial distributions. But a number of uncertainties remain when assessing potential changes of fire-weather risk associated with climate change. Fuel, weather and topography are the main variables influencing fire behavior. Fuel types were assumed to be constant between scenarios although vegetation types, and hence, fuel types might change as result of climate warming. Actually, if the climate changes, the forest belt in northeast China will tend to move northward, and temperate broadleaved-coniferous mixed forest would become dominant (Cheng et al. 2007). The other uncertainties relate to the quality of data for some weather variables, the possibility of different results from the other climate models, ignition and fuel load changes, and extreme weather events under climate change (Hennessy et al. 2005). To improve our ability to better predict wildfire, future research should focus on incorporating additional effects of long-term and successional vegetation changes on area burned to account more fully for interactions among fire, climate and vegetation dynamics (Balshi et al. 2008).

Although there will be large spatial and temporal variation in the fire activity response to climate change, this research enables us to better understand the interactions and feedbacks between fire, climate, vegetation and humans and to identify vulnerable regions (Flannigan et al. 2005). Since the capacity is limited among fire management agencies to cope with increased fire activity, we expect that the successful initial responses will decrease under a warmer climate and this will result in an increase in area burned that will be much greater than the corresponding

increase in fire weather severity (Flannigan et al. 2009). There may be only a decade or two before sharp increases in fire activity and this means that fire management agencies will not be able to maintain their current levels of effectiveness in future (Flannigan et al. 2009).

The fire regime will be changed because of climate change. Fire management needs to be adjusted in terms of budget, personnel, technology, equipment, early warning, and monitoring systems if it is to successfully adapt. According to changes of fire danger and fire season in the future, we suggest to strengthen early warning and monitoring, pay attention to post-fire recovery, and use prescribed burning and other adaptive management measures. In the east, it is necessary to use prescribed burning, manual or mechanical cleaning, and the other methods to reduce flammable loads and adapt to climate change.

References

Amiro BD, Cantin A, Flannigan MD, de Groot W. 2009. Future Emissions from Canadian Boreal Forest Fires. *Canadian Journal of Forest Research*, **39**: 383−395.

Balshi MS, McGuire AD, Duffy P, Flannigan M, Walsh J, Melillo J. 2008.Assessing the response of area burned to changing climate in western boreal North America using a Multivariate Adaptive Regression Splines (MARS) approach. *Global Change Biology*, **15**: 578−600.

Carvalho A, Flannigan M, Logan K, Gowman L, Miranda A, Borrego C. 2010. The impact of spatial resolution on area burned and fire occurrence projections in Portugal under climate change, *Climatic Change*, **98**(1/2): 177197.

Cheng Xiaoxia, Yan Xiaodong. 2007. Efects of global climate change on forest succession in Daxing'anling of Northeast China. *Chinese Journal of Ecology*, **26**(8):1277–1284. (in Chinese)

Drever CR, Bergeron Y, Drever MC, Flannigan M, LoganT, Messier C. 2009. Effects of climate on occurrence and size of large fires in a northern hardwood landscape: historical trends, future predictions, and implications for climate change in Témiscamingue, Québec. *Applied Vegetation Science*, **12**: 261−272.

Flannigan MD, Logan KA, Amiro BD, Skinner WR, Stocks BJ. 2005. Future area burned in Canada. *Climatic Change*, **72**:1−16

Flannigan MD, Krawchuk MA, de Groot WJ, Wotton BM, Gowman LM. 2009. Implications of changing climate for global wildland fire. *International Journal of Wildland Fire*, **18**(5): 483−507.

Flannigan MD, Stocks BJ, Turetsky MR, Wotton BM. 2009. Impact of climate change on fire activity and fire management in the circumboreal forest. *Global Change Biology*, **15**: 549−560.

Gao Yonggang, Zhange Guangying, Gu Hong, Zhou Erbin. 2008. Influences of climatic change on forest fire in Yichun forest region. *Journal of Anhui Agricultural Science*, **36**(28): 12269−12271, 12274. (in Chinese)

Hennessy KJ, Lucas C, Nicholls N, Bathols JM, Suppiah R, Ricketts JR. 2005. Climate change impacts on fire-weather in south-east Australia. Consultancy report by CSIRO Marine and Atmospheric Research, Bureau of Meteorology and Bushfire CRC. pp.88. http://www.cmar.csiro.au/e-print/open/hennessykj_2005b.pdf

Hutchinson MF. 1998. Interpolation of rainfall data with thin plate smoothing splines - Part I: two dimensional smoothing of data with short range correlation. *Journal of Geographic Information and Decision Analysis*, **2**(2): 152−167

Johnes RG, Noguer M, Hassell DC. 2004. Generating high resolution climate change scenations using PRECIS. UK: Met office Hadley Centre, Exeter.

Kochtubajda B, Flannigan MD, Gyakum JR, Stewart RE, Logan KA, Nguyen TV. 2006. Lightning and fires in the northwest territories and responses to future climate change. *Arctic*, **59**(2): 211−221.

Le Goff H, Flannigan M, Bergeron Y. 2009. Potential changes in monthly fire risk in the eastern Canadian boreal forest under future climate change. *Canadian Journal of Forest Research*, **39**(12): 2369−2380.

Lynham TJ, Stocks BJ. 1989. Suitability of the Canadian forest fire danger ranting system for use in the Daxingangling forestry management Bureau Heilongjiang Province, China. 10th Conference on Fire and Forest Meteorology, Ottawa, Canada.

Spittlehouse DL, Stewart RB. 2003. Adaptation to climate change in forest management. *Journal of Ecosystems and Management*, **4**(1): 1−11.

Qin Dahe, Ding Yihui, Wu Rongsheng, Yang Xiuqun, Wang Sumin, Liu Shiyin, Dong Gunagrong, Lu Qi, Huang Zhenguo, Du Bilan, Luo Yong. 2005. Assessment of climate and environment changes in China (I): Climate and environment changes in China and their projection. *Advances in Climate Change Research*, **1**(1): 4−9. (in Chinese)

Soja AJ, Tchebakova NM, French NH, Flannigan MD, Shugart HH, Stocks BJ, Sukhinin AI, Parfenova, EI, Chapin T. 2006. Climate-induced boreal forest change: predictions versus current observations. *Global and Planetary Change*, **56**(3/4): 274−296.

Spracklen DV, Mickley LJ, Logan JA, Hudman RC, Yevich R, Flanning MD, Westerling AL. 2009. Impacts of climate change from 2000 to 2050 on wildfire activity and carbonaceous aerosol concentrations in the western United States. *Journal of Geophysical Research*, **114**, D20301, DOI:10.1029/2008JD010966.

Stocks BJ, Lawson BD, Alexander ME, Van Wagner CE, Alpine RS, Lynham TJ, Dube DE. 1989. The Canadian forest fire danger rating system: an overview. *Forestry Chronicle*, **65**(4): 450–457.

Sun Fenghua, Yuan Jian, Lu Shuang. 2006. The Change and Test of Climate in Northeast China over the Last 100 Years. *Climatic and Environmental Research*, **11**(1):101–108. (in Chinese)

Tang Guoli, Ren Guoyu. 2005. Reanalysis of surface air temperature change of the last 100 years over China. *Climatic and Environmental Research*, **l0**(4): 791–798. (in Chinese)

Tian Xiaorui, McRae DJ, Jin Jizhong, Shu Lifu, Zhao Fengjun, Wang Mingyu. 2010. Changes of Forest Fire Danger During 1987-2006 in the Daxing'anling region. *Scientia Silvae Sinicae*, **46**(5): 127–132. (in Chinese)

Tian Xiaorui, Shu Lifu, Wang Mingyu, Zhao Fengjun. 2009. Spatial and Temporal Distribution of Lightning Fire and Forecasting Model for Daxing'anling Region. *Forest Research*, **22**(1): 14–20. (in Chinese)

Tymstra C, Flannigan M, Armitage B, Logan K. 2007. Impact of climate change on area burned in Alberta's boreal forest. *International Journal of Wildland Fire*, **16**(2): 153−160.

Weber MG, Flannigan MD. 1997. Canadian boreal forest ecosystem structure and function in a changing climate: Impacts on fire regimes. *Environ Review*, **5**: 145−166.

Williams AAJ, Karoly DJ, Tapper N. 2001. The sensitivity of Australian fire danger to climate change. *Climate Change*, **49**(1/2): 171–191.

Wotton BM, Martell DL, Logan KA. 2003. Climate change and people-caused forest fire occurrence in Ontario. *Climatic Change*, **60**(3): 275–295.

Wotton BM, Nock CA, Flannigan MD. 2010. Forest fire occurrence and

climate change in Canada. *International Journal of Wildland Fire*, **19**(3): 253–271.

Xu Yinlong, Zhang Yong, Lin Yihua, Lin Erda, Lin Wantao, Dong Wenjie, Jones R, Hassell D, Wilson S. 2006. Validating PRECIS analyses on scenario of SRES B2 over China. *Chinese Science Bulletin*, **51**(17): 2068–2074. (in Chinese)

Yang Guang, Di Xueying, Zeng Tao, Shu Zhan, Wang Chao, Yu Hongzhou. 2010. Prediction of area burned under climatic change scenarios: A case study in the Great Xing'an Mountains boreal forest. *Journal of Forestry Research*, **21**(2): 213–218.

Zhao Fengjun, Shu Lifu, Di Xueying, Tian Xiaorui, Wang Mingyu. 2009. Changes in the occurring date of forest fires in the Inner Mongolia Daxing'anling forest region under global warming. *Scientia Silvae Sinicae*, **45**(6): 166–172. (in Chinese)

Zhong Chongqi. 1990. Forestry site of Northeast China. Harbin: Northeast Forestry University Press, p 1–5. (in Chinese)